Perturbative calculation of transition amplitudes for cesium

S. S. Liaw*
Department of Physics, National Chung-Hsing University, 250, Guo-Kwang Road, Taichung, Taiwan
(Received 25 September 1992)

We have done a many-body-perturbation-theory calculation, up to second order, for $6s \rightarrow 6p_{1/2}$ and $6s \rightarrow 6p_{3/2}$ transitions for Cs using the Dirac-Fock orbitals as single-particle wave functions. The results show that many-body-perturbation-theory calculations for transition amplitudes do not converge well unless some infinite subsets of diagrams are included. A systematic way of including infinite subsets of diagrams based on the Green's-function formalism that preserves gauge invariance of transition amplitudes in each step is proposed for future work.

PACS number(s): 32.70.Cs, 31.10.+z

I. INTRODUCTION

The accurate measurement [1] of the parity violation in Cs has raised the interest of atomic theorists to do precision calculation for heavy atoms. Among the techniques that are in current use, the many-body-perturbation-theory (MBPT) calculation [2] has a particular attraction. Namely, one can in principle improve the accuracy step by step by including more and more diagrams. The fast increasing power of computers helps in making the calculations possible. The question is, then, how much effort should be made if a certain accuracy is needed. The answer, of course, depends on how well the calculation converges order by order. In the case of energy levels of low bound states of alkali-metal atoms, the MBPT calculation has been shown to converge very well [3]. An accuracy of better than 1% is obtained for Cs in the MBPT calculation including up to third order [4].

In this article, we carry out the MBPT calculation for transition amplitudes up to second order for $6s \rightarrow 6p_{1/2}$ and $6s \rightarrow 6p_{3/2}$ transitions in Cs. We found, however, that the results converge poorly, in particular for the velocity form. The agreement between length and velocity forms is not improved as one goes from lowest to second order. By comparison with other similar calculations [5,6], we see that the inclusion of infinite subsets of diagrams is essential to obtain good results for the transition amplitudes. The plan of this article is as follows. In Sec. II formulas for transition amplitudes up to second order are given. The numerical method and results are presented in Sec. III. In Sec. IV we compare present calculation with two other similar calculations, and propose a systematic calculation for future work. A simple recipe for "reading" explicit algebraic expression from diagrams is given in the Appendix.

FIG. 1. Local Dirac-Fock vertex.

II. FORMULAS FOR TRANSITION AMPLITUDES

One can derive the expression for transition amplitudes order by order from either the MBPT or the Green's-function formalism [7]. The Dirac-Fock approximation (DFA) is a natural starting point from the point of view of Green's-function formalism. The Dirac-Fock (DF) wave functions are also the simplest choice (except hydrogenlike ones) for initial single-particle wave functions in the MBPT. Based on either formalism, the transition amplitudes of a given order can be represented by their corresponding Feynman diagrams. Let a solid line represent the electron propagator in the DFA, a dotted line represent electron-electron interaction V, and a cross ($\times$) represent the local three-point vertex. The local transition amplitude in the DFA is represented by Fig. 1. The first-order (that is, one-V-line) corrections are represented by Fig. 2. The second-order (that is, two-V-line) corrections are represented by Figs. 3(a)–3(c). If we denote the matrix element between two arbitrary DF states $|s\rangle$ and $|t\rangle$ as u_{st}, the local transition amplitude between two valence states $|m\rangle$ and $|n\rangle$ in the DFA (Fig. 1) is simply u_{nm}. Explicitly,

$$Z^{\mathrm{DF}} = u_{nm} = \sum_M (-1)^{j_n - m_n} \begin{pmatrix} j_n & 1 & j_m \\ -m_n & M & m_m \end{pmatrix} D_{nm} , \qquad (1)$$

where D_{nm} is the reduced dipole matrix element. The explicit expressions corresponding to the first- and second-order diagrams [Figs. 2 and 3(a)–3(c)] can be put in the following form:

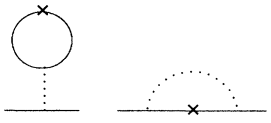

FIG. 2. First-order correction to the local Dirac-Fock vertex.

$$Z^{(1)}=(+1)\sum_{a,i}\frac{1}{\varepsilon_n-\varepsilon_m+\varepsilon_a-\varepsilon_i}[\langle an|V|im\rangle]u_{ia}+\text{c.c.}\ , \tag{2}$$

$$Z^{(2)}_{3(a)}=(-\tfrac{1}{2})\sum_{a,i,j,s}\frac{1}{\varepsilon_m-\varepsilon_s}\frac{1}{\varepsilon_m+\varepsilon_a-\varepsilon_i-\varepsilon_j}[\langle sa|V|ij\rangle][\langle ij|V|am\rangle]u_n+\text{c.c.}$$
$$+(-\tfrac{1}{2})\sum_{a,b,i,s}\frac{1}{\varepsilon_m-\varepsilon_s}\frac{1}{\varepsilon_m-\varepsilon_a-\varepsilon_b+\varepsilon_i}[\langle si|V|ab\rangle][\langle ab|V|im\rangle]u_{ns}+\text{c.c.}\ , \tag{3}$$

$$Z^{(2)}_{3(b)}=(-1)\sum_{a,i,j,k}\frac{1}{\varepsilon_n+\varepsilon_a-\varepsilon_i-\varepsilon_k}\frac{1}{\varepsilon_m+\varepsilon_a-\varepsilon_j-\varepsilon_k}[\langle na|V|ik\rangle][\langle jk|V|am\rangle]u_{ij}$$
$$+(-1)\sum_{a,b,c,i}\frac{1}{\varepsilon_m-\varepsilon_b-\varepsilon_c+\varepsilon_i}\frac{1}{\varepsilon_n-\varepsilon_a-\varepsilon_c-\varepsilon_i}[\langle ni|V|ac\rangle][\langle bc|V|im\rangle]u_{ab}$$
$$+(+1)\sum_{a,b,i,j}\frac{1}{\varepsilon_n-\varepsilon_m+\varepsilon_a-\varepsilon_i}\frac{1}{\varepsilon_n+\varepsilon_b-\varepsilon_i-\varepsilon_j}[\langle nb|V|ij\rangle][\langle aj|V|bm\rangle]u_{ia}+\text{c.c.}$$
$$+(-1)\sum_{a,b,i,j}\frac{1}{\varepsilon_m-\varepsilon_a-\varepsilon_b+\varepsilon_j}\frac{1}{\varepsilon_n-\varepsilon_m+\varepsilon_a-\varepsilon_i}[\langle nj|V|ib\rangle][\langle ab|V|jm\rangle]u_{ia}+\text{c.c.}$$
$$+(+\tfrac{1}{2})\sum_{a,b,i,j}\frac{1}{\varepsilon_m-\varepsilon_a-\varepsilon_b+\varepsilon_i}\frac{1}{\varepsilon_n-\varepsilon_a-\varepsilon_b+\varepsilon_j}[\langle nj|V|ba\rangle][\langle ba|V|im\rangle]u_{ij}$$
$$+(+\tfrac{1}{2})\sum_{a,b,i,j}\frac{1}{\varepsilon_n+\varepsilon_b-\varepsilon_i-\varepsilon_j}\frac{1}{\varepsilon_m+\varepsilon_a-\varepsilon_i-\varepsilon_j}[\langle nb|V|ij\rangle][\langle ij|V|am\rangle]u_{ab}$$
$$+(-\tfrac{1}{2})\sum_{a,i,j,k}\frac{1}{\varepsilon_n+\varepsilon_a-\varepsilon_j-\varepsilon_k}\frac{1}{\varepsilon_n-\varepsilon_m+\varepsilon_a-\varepsilon_i}[\langle na|V|jk\rangle][\langle jk|V|im\rangle]u_{ia}+\text{c.c.}$$
$$+(+\tfrac{1}{2})\sum_{a,b,c,i}\frac{1}{\varepsilon_m-\varepsilon_b-\varepsilon_c+\varepsilon_i}\frac{1}{\varepsilon_n-\varepsilon_m+\varepsilon_a-\varepsilon_i}[\langle na|V|bc\rangle][\langle bc|V|im\rangle]u_{ia}+\text{c.c.}\ , \tag{4}$$

$$Z^{(2)}_{3(c)}=(+1)\sum_{a,b,i,j}\frac{1}{\varepsilon_n-\varepsilon_m+\varepsilon_a-\varepsilon_i}\frac{1}{\varepsilon_n-\varepsilon_m+\varepsilon_b-\varepsilon_j}[\langle nb|V|jm\rangle][\langle ja|V|ib\rangle]u_{ia}+\text{c.c.}$$
$$+(+1)\sum_{a,b,i,j}\frac{1}{\varepsilon_n-\varepsilon_m+\varepsilon_a-\varepsilon_i}\frac{1}{\varepsilon_m-\varepsilon_n+\varepsilon_b-\varepsilon_j}[\langle nj|V|bm\rangle][\langle ba|V|ij\rangle]u_{ia}+\text{c.c.}\ , \tag{5}$$

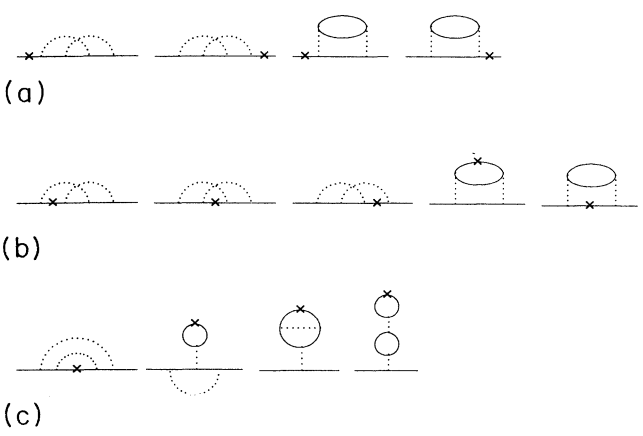

FIG. 3. (a) Part of the second-order corrections. These diagrams were computed in Ref. [5]. They are included in the first-order local vertex if Brueckner orbitals are used. (b) Part of the second-order corrections. These diagrams were not computed in either Ref. [5] or [6]. (c) Part of the second-order corrections. These diagrams are included in the gauge-invariant Dirac-Fock transition amplitudes (Fig. 4).

where

$$\langle mn|V|st\rangle=\int\phi^{\dagger}_m(\mathbf{r}_1)\phi^{\dagger}_n(\mathbf{r}_2)V(\mathbf{r}_1-\mathbf{r}_2)\times\phi_s(\mathbf{r}_1)\phi_t(\mathbf{r}_2)d\mathbf{r}_1d\mathbf{r}_2 \tag{6}$$

and the bracket [ ] denotes antisymmetrization, i.e.,

$$[\langle mn|V|st\rangle]\equiv\langle mn|V|st\rangle-\langle mn|V|ts\rangle\ . \tag{7}$$

In the above expressions m and n refer to two valence states, and the c.c. notation means that the previous term is to be complex conjugated and that the roles of m and n are to be interchanged. The sum over the index s in Eq. (3) ranges over all states except for the valence state. The indices a, b, and c stand for DF hole states (a core minus one electron), and their corresponding sums range over the core. The indices i, j, and k stand for particle states (a core plus one electron), and their corresponding sums range over all positive states outside the core. ε is the DF energy of the state indicated by its subscript.

A simple recipe is given in the Appendix to read out the expression from its corresponding diagram. The second-order formulas have also been given in Ref. [5] by Johnson, Idrees, and Sapirstein and are called the third-order contributions there.

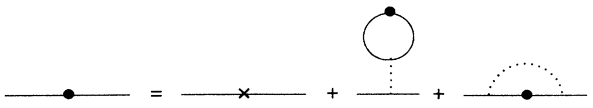

FIG. 4. The gauge-invariant Dirac-Fock transition amplitudes.

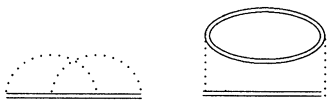

FIG. 5. The second-order self-energy diagrams.

III. METHOD OF CALCULATION AND RESULTS

The angular parts of the expressions in Eqs. (2)–(5) can be summed analytically to be in the form of 3-j, 6-j, or 9-j coefficients. They are then computed by computer. For the radial parts, we use the B-spline approximation for the complete DF wave functions [8]. For each s, $p_{1/2}$, $p_{3/2}, \ldots, i_{11/2}$, and $i_{13/2}$ state, we generate a pseudospectrum with 40 positive-energy and 40 negative-energy states. The first 33 (counting from the lowest-energy state up) positive-energy wave functions and their corresponding energy levels are then used in calculation. The results are presented in Table I. The final results of length form differ from experimental values [9] by 6% and 12% for the $6s \rightarrow 6p_{1/2}$ and $6s \rightarrow 6p_{3/2}$ transitions, respectively. The results of velocity form are in better agreement with experimental values.

Figure 3(a) has also been calculated by Johnson, Idrees, and Sapirstein [5] using the same method. Because they used Aitken's extrapolation to get the final value, their values differ from ours a little bit (see column 5, Table II).

One notices that the second-order contribution [Fig. 3(a) plus 3(b) plus 3(c)] is either comparable with or larger than the first-order contribution. The perturbative series apparently converges poorly. One cannot have an idea of what size the third-order contribution is going to be. We can also see from Table I that the length and velocity forms of the transition amplitudes are not the same. They differ by 5% in local values. Including perturbative corrections up to second order does not improve the agreement at all.

IV. DISCUSSION AND COMPARISON WITH OTHER CALCULATIONS

In order to compare our results with other similar calculations, we have to mention briefly an alternative way of calculating transition amplitudes "order by order." The method has been proposed by Feldman and Fulton from the Green's-function formalism [10]. In this method, one systematically sums a subset of infinite number of diagrams in a manner so that the transition amplitude is gauge invariant in each step. The lowest-order diagram of each subset is an irreducible self-energy diagram. The first- and second-order self-energy diagram are given in Figs. 2 and 3(b), respectively.

The zeroth-order approximation is the independent particle approximation. The transition amplitude is certainly gauge invariant. The first-order approximation is the well-known DFA. Based on the formalism, Feldman and Fulton [10] showed that the gauge-invariant transition amplitudes in the DFA is not given by Fig. 1. They found that the transition amplitudes satisfy a self-consistent equation represented by Fig. 4, which contains local contribution (Fig. 1) and nonlocal contribution due to the first-order self-energy diagrams (Fig. 2 and corresponding higher-order diagrams). By iteration starting from the first term on the right-hand side (rhs) of Fig. 4 (namely, the local contribution), one can generate an infinite set of diagrams. The difference between this gauge-invariant transition amplitudes and the local contribution is sometimes called the random-phase-approximation (RPA) -type contribution [11]. A few numerical results for Fig. 4 have been presented [11,12].

The next step is the second-order approximation. In this approximation, the wave functions have to be solved by including second-order self-energy diagrams (Fig. 5). The double line in Fig. 5 is the electron propagator under this approximation. These wave functions are sometimes called Brueckner orbitals [13]. The gauge-invariant transition amplitudes in this approximation can be inferred from the work of Feldman and Fulton [10]. Diagrammatically, it is given by Fig. 6. Note that Fig. 6, like Fig. 4, is a self-consistent integral equation for the transition amplitude. This equation has not been solved yet.

Having briefly presented the gauge-invariant approach to transition amplitudes from the Green's-function formalism, we are in a position to discuss the work done by Johnson, Idrees, and Sapirstein [5] and Dzuba *et al.* [6]. We hereafter refer to them as I and II, respectively.

TABLE I. Reduced dipole matrix elements for the resonance transitions $6s \rightarrow 6p_{1/2,3/2}$ in Cs.

		Local DF	First order	Second order				
Transition	Form	Fig. 1	Fig. 2	Fig. 3(a)	Fig. 3(b)	Fig. 3(c)	Sum	Expt.[a]
	length	5.278	−0.334	−0.577	0.044	0.377	4.788	
$6s \rightarrow 6p_{1/2}$	velocity	5.036	−0.207	−0.560	0.051	0.234	4.554	4.52
	length	−7.426	−0.005	0.836	−0.059	−0.504	−7.158	
$6s \rightarrow 6p_{3/2}$	velocity	−7.064	−0.002	0.807	−0.053	−0.313	−6.625	−6.36

[a]Reference [9].

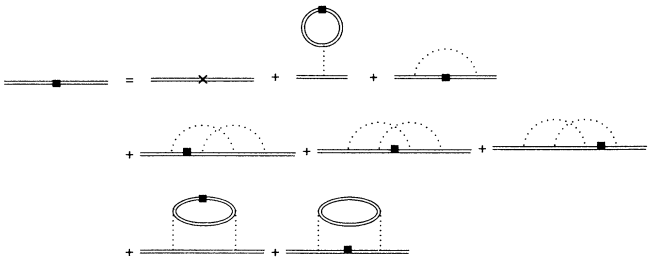

FIG. 6. A gauge-invariant transition amplitudes including up to second-order self-energy diagrams.

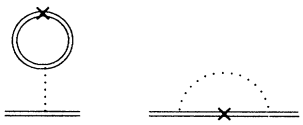

FIG. 7. First-order corrections to the local transition amplitudes when using Brueckner orbitals.

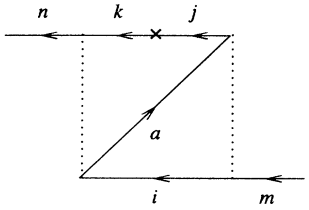

FIG. 8. A second-order Heitler diagram where time order is explicitly shown.

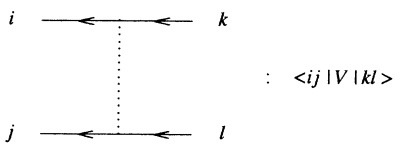

FIG. 9. Diagrammatic representation of the matrix element $\langle ij|V|kl\rangle$.

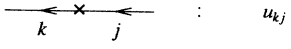

FIG. 10. Diagrammatic representation of the matrix element u_{kj}.

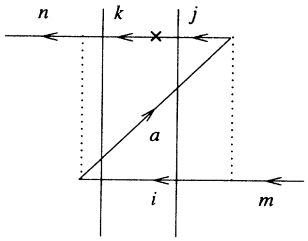

FIG. 11. A Heitler diagram with two auxiliary lines to help in reading out its corresponding algebraic expression.

I used DF orbitals and calculated RPA-type contributions of transition amplitudes according to Fig. 4, which certainly included the first-order polarization correction (Fig. 2). They then added part of the second-order corrections, namely, the contribution from Fig. 3(a). The part of the second-order contributions from Fig. 3(c) has been included in Fig. 4, while that from Fig. 3(b) is claimed to be an order smaller than that from Fig. 3(a) by energy-denominator consideration and is not calculated. Their calculation is a combination of the perturbative calculation presented in Sec. II and the gauge-invariant method described in the beginning of this section. They are able to get a final result of 3% difference with experimental value. We list their results in Table II. The velocity forms also shown in Table II are calculated by us for comparison. If the corrections from Fig. 3(b) were included (column 7, Table II), their results would have been closer to experimental value (within 2% error).

In the work of II, Dzuba *et al.* first obtained the Brueckner orbitals with a few approximations for convenience without changing the accuracy needed. For transition amplitudes, they then calculated the first term of the right-hand side of Fig. 6, which automatically includes the contributions from Fig. 3(a). They then added the first-order perturbative corrections (core polarization) corresponding to the diagrams shown in Fig. 7. Note that Fig. 7 is the same as Fig. 2 except that the DF orbitals are replaced by the Brueckner orbitals. They claimed that the high-order RPA-type contribution is small and did not present it in their results. We estimate this RPA-type correction using the DF orbitals by taking the difference of the contributions from column 4, Table II and column 4, Table I. We obtain for the $6s \rightarrow 6p_{1/2}$ transition $-0.303-(-0.334)=0.031$ (length form) and $-0.063-(-0.207)=0.144$ (velocity form). These values are 0.7% and 3.1% of the experimental value, respectively. The part of second-order contributions from the last five diagrams of the right-hand side of Fig. 6 is also neglected in their work. This part of second-order contributions can be approximated by Fig. 3(b) using the DF orbitals; it is 0.044 (length form) and 0.051 (velocity form) given in Table I. They are about 1% of experimental value. With these estimated corrections (column 5, Table III), the results of II are brought closer to the experimental value for the length form (less than 0.5% error). But, based on the results of II, our estimated correction for the velocity form is apparently not good.

TABLE II. Results of Johnson, Idrees, and Sapirstein for the transitions $6s \rightarrow 6p_{1/2,3/2}$. Column 7 gives estimated corrections to their results based on our calculation. Values in velocity form are calculated by us.

Transition		Local DF[a] (Fig. 1)	RPA[a] (Fig. 4)	Second order[a] [Fig. 3(a)]	Sum[a]	Correction[b] [Fig. 3(b)]	Expt.[c]
	length	5.278	−0.303	−0.582	4.393	0.044	
$6s \rightarrow 6p_{1/2}$	velocity	5.036	−0.063	−0.560	4.413	0.051	4.52
	length	−7.426	0.413	0.842	−6.171	−0.059	
$6s \rightarrow 6p_{3/2}$	velocity	−7.064	0.053	0.807	−6.204	−0.053	−6.36

[a]Reference [5].
[b]Present calculation.
[c]Reference [9].

The possible reason is that since the high-order RPA-type correction using the DF orbitals is quite large (3.1%), we would expect that this value would be changed significantly if the Brueckner orbitals are used instead. In addition, the high-order (order 3 and up) contribution generated from Fig. 3(b) can be also large. Therefore our estimated corrections for the velocity form are not suitable. The equation represented by Fig. 6 should be solved to get a better result.

From the perturbative point of view (Sec. II), up to second order, I neglects the contributions form Fig. 3(b), while II drops out the contributions from Figs. 3(b) and 3(c). However, as we have seen in Sec. III, the perturbative calculation order by order does not converge well anyway. Instead, we see that, by including an infinite subset of diagrams, for example, the RPA-type contribution in I or using the Brueckner orbitals in II, we can get better theoretical results. The question is which subsets of diagrams are more important to be included for obtaining good results for transition amplitudes in whatever gauge. Fortunately, the Green's-function formalism give us a systematic way to sum over the infinite subsets of diagrams order by order as we have sketched in the beginning of this section. The formalism also guarantees that the resultant transition amplitudes are gauge invariant order by order. We will demonstrate this assertion explicitly in future work.

Recently, there are also some "all-order" calculations along this line [14,15]. Since these works are somewhat beyond the scope of this paper, the comparison with them will be more appropriately done in our future work based on the Green's-function formalism.

ACKNOWLEDGMENTS

This work is supported in part by the National Science Council of the Republic of China under Grant No. NSC 82-0208-M-005-051.

APPENDIX

Given a Feynman diagram, say, the first diagrams in Fig. 3(b), there are six time-ordered diagrams corresponding to it. They are called Heitler diagrams. One of these Heitler diagrams is shown by Fig. 8. In Fig. 8 we have shown the time direction of the DF propagator explicitly, assuming initial and final valence states are $|m\rangle$ and $|n\rangle$, respectively. Let us use this Heitler diagram as an example for explaining the rule to write down the algebraic expression.

An algebraic expression consists of three parts: numerator, denominator, and phase. They can be read from the corresponding Heitler diagram according to the following rules.

(1) Designate each DF propagator either by a particle label if it propagates forward (in time) or by a hole label if backward.

(2) Associate each electron-electron interaction V and the three-point vertex $\times$ with a matrix element such as $\langle ij|V|kl\rangle$ for Fig. 9 and u_{kj} for Fig. 10. The numerator is the product of these matrix elements. For example, for diagrams Fig. 8, the numerator is given by

$$\langle na|V|ki\rangle\langle ji|V|am\rangle u_{kj} .$$

(3) Draw lines through the Heitler diagram between

TABLE III. Results of Dzuba *et al.* for the transition $6s \rightarrow 6p_{1/2}$. Column 5 gives estimated corrections to their results based on our calculation.

	Local Brueckner[a] (first term on rhs of Fig. 6)	First order[a] (Fig. 7)	Sum[a]	Correction[b] [Fig. 3(b) + Fig. 4 − Fig. 2]	Expt.[c]
length	4.82	−0.37	4.45	0.075	4.52
velocity	4.63	−0.07	4.56	0.195	

[a]Reference [6].
[b]Present calculation.
[c]Reference [9].

each time interval as shown in Fig. 11 for the case of Fig. 8. For each line, assign an energy factor according to what propagators it intersects as follows: If the line is before the vertex (in time), we have

$$\varepsilon_m - (\text{energies of particles}) + (\text{energies of holes}) .$$

If the line is after the vertex, replace ε_m by ε_n. The energy denominator is the product of these energy factors. For example, for diagram Fig. 11 we get the energy denominator

$$(\varepsilon_n - \varepsilon_i - \varepsilon_k + \varepsilon_a)(\varepsilon_m - \varepsilon_i - \varepsilon_j + \varepsilon_a) .$$

(4) The phase is determined by h, the number of propagators labeled by holes, and l the number of fermion (electron) loops. It is given by

$$(\text{phase}) = (-1)^{h+l} .$$

For example, for diagram Fig. 8 the phase is given by

$$(-1)^{1+0} = -1 .$$

The final algebraic result according to these rules for the Heitler diagram Fig. 8 is

$$\sum_{a,i,j,k} (-1) \frac{1}{(\varepsilon_n - \varepsilon_i - \varepsilon_k + \varepsilon_a)} \frac{1}{(\varepsilon_m - \varepsilon_i - \varepsilon_j + \varepsilon_a)} \times \langle na | V | ki \rangle \langle ji | V | am \rangle u_{kj} .$$

Hole states are to be summed over the core, and particle states are to be summed and integrated over states outside the core.

*Electronic address: liaw@phys2.nchu.edu.tw

[1] M. A. Bouchiat, J. Guena, L. Hunter, and L. Pottier, Phys. Lett. **134B**, 463 (1984).
[2] See, for example, I. Lindgren and J. Morrison, *Atomic Many-Body Theory,* 2nd ed. (Springer-Verlag, Berlin, 1986).
[3] V. A. Dzuba, V. V. Flambaum, and O. P. Sushkov, J. Phys. B **16**, 715 (1983).
[4] S. A. Blundell, W. R. Johnson, and J. Sapirstein, Phys. Rev. A **42**, 3751 (1991).
[5] W. R. Johnson, M. Idrees, and J. Sapirstein, Phys. Rev. A **35**, 3218 (1987).
[6] V. A. Dzuba, V. V. Flambaum, P. G. Silvestrov, and O. P. Sushkov, J. Phys. B **18**, 597 (1985).
[7] Gy. Csanak, H. S. Taylor, and R. Yaris, Adv. At. Mol. Phys. **7**, 287 (1971).
[8] W. R. Johnson, S. A. Blundell, and J. Sapirstein, Phys. Rev. A **37**, 307 (1988).
[9] L. Shabanova, Yu. Monukov, and A. Khlyustalov, Opt. Spektrosk. **47**, 3 (1979) [Opt. Spectrosc. (USSR) **47**, 1 (1979)].
[10] G. Feldman and T. Fulton, Ann. Phys. (N.Y.) **152**, 376 (1984); **172**, 40 (1986).
[11] T. Fulton and W. R. Johnson, Phys. Rev. A **34**, 1686 (1986).
[12] S. S. Liaw, Can. J. Phys. **70**, 644 (1992).
[13] See, for example, I. Lindgren, J. Lindgren, and A.-M. Mårtensson, Z. Phys. A **279**, 113 (1976).
[14] V. A. Dzuba, V. V. Flambaum, and O. P. Sushkov, Phys. Lett. **142**, 373 (1989).
[15] S. A. Blundell, W. R. Johnson, and J. Sapirstein, Phys. Rev. A **43**, 3407 (1991).